BIOCHEMISTRY
including biophysical chemistry & molecular biology
Article

Biochemistry **2009,** *48,* 8261–8270 8261
DOI: 10.1021/bi900921t

Mutagenesis Studies toward Understanding Allostery in Thrombin[†]

Shabir H. Qureshi,[‡] Likui Yang,[‡] Chandrashekhara Manithody,[‡] Alexei V. Iakhiaev,[§] and Alireza R. Rezaie*[,‡]

[‡]*Edward A. Doisy Department of Biochemistry and Molecular Biology, Saint Louis University School of Medicine, Saint Louis, Missouri 63104, and* [§]*Texas College, Tyler, Texas 75702-4500*

Received June 2, 2009; Revised Manuscript Received July 28, 2009

ABSTRACT: The binding of thrombomodulin (TM) to exosite-1 and the binding of Na^+ to 225-loop allosterically modulate the catalytic activity and substrate specificity of thrombin. To determine whether the conformation of these two cofactor-binding loops are energetically linked to each other and to the active site, we rationally designed two thrombin mutants in which either the 70−80 loop of exosite-1 or the 225-loop of the Na^+-binding site was stabilized by an engineered disulfide bond. This was possible by replacing two residues, Arg-67 and Ile-82, in the first mutant and two residues, Glu-217 and Lys-224, in the second mutant with Cys residues. These mutants were expressed in mammalian cells as monomeric molecules, purified to homogeneity and characterized with respect to their ability to bind TM and Na^+ by kinetic and direct binding approaches. The Cys-67/Cys-82 mutant did not bind TM and exhibited a normal amidolytic activity, however, the activity of Cys-217/Cys-224 was dramatically impaired, though TM interacted with this mutant with >20-fold elevated K_D to partially restore its activity. Both mutants exhibited ∼2−3-fold higher K_D for interaction with Na^+, and neither mutant clotted fibrinogen or activated protein C in the presence of TM. Both mutants interacted with heparin with a normal affinity. These results suggest that, while exosite-2 of thrombin is an independent cofactor binding-site, both Na^+-binding and exosite-1 are energetically linked. Further studies with the fluorescein labeled Cys-195 mutant of thrombin revealed that the catalytic residue of thrombin is modulated by Na^+, but TM has no effect on the conformation of this residue.

Thrombin is an allosteric trypsin-like serine protease in plasma that is responsible for clotting fibrinogen and up-regulating the clotting cascade by activating platelets, cofactors V and VIII, and factor XIII during injury to blood vessels (*1*−*5*). Thrombin also down-regulates its own production by a negative feed back loop mechanism when it binds to endothelial cell surface glycoprotein thrombomodulin (TM[1]) to activate protein C to activated protein C (APC), thereby initiating the anticoagulant pathway (*6*−*9*). APC inhibits thrombin generation by proteolytically degrading the activated forms of factors V and VIII, which are essential cofactors for the prothrombinase and intrinsic Xase complexes, respectively (*10*). The proteolytic activity of thrombin is primarily regulated by the plasma serpin antithrombin (AT) which functions as a pseudosubstrate to trap the protease in the form of an inactive and irreversible acylated complex incapable of interacting with any true substrate (*11*). Structural and mutagenesis data have indicated that several different ligands bind to distinct loops removed from the active site (exosite) to allosterically modulate the substrate specificity of thrombin, thereby rendering the protease capable of selecting its distinct substrates and cofactors in the opposite procoagulant and anticoagulant pathways (*5*, *12*, *13*). Thus, it has been demonstrated that the epidermal growth factor (EGF)-like domains 4−6 of thrombomodulin (TM4−6) switch the substrate specificity of thrombin by binding to exosite-1 of the protease, thereby competitively inhibiting the binding of fibrinogen to this site and, at the same time, improving the catalytic activity of thrombin toward its substrate protein C in the anticoagulant pathway (*14*−*17*). The mechanism by which TM improves the catalytic efficiency of thrombin toward protein C is incompletely understood. In addition to TM, the substrate specificity of thrombin is also modulated by the monovalent cation Na^+ binding to the 217−225-loop (designated 225-loop, chymotrypsin numbering system (*18*)), immediately below the primary S1 specificity pocket (nomenclature of Schechter and Berger (*19*)). Nevertheless, because of the high dissociation constant for Na^+, thrombin exists in equilibrium between Na^+-bound (fast) and Na^+-free (slow) conformers under a physiological concentration of Na^+ and temperature (*4*). It has been established that the fast form of thrombin primarily functions in the procoagulant pathway by being capable of cleaving fibrinogen with a high catalytic efficiency (*4*). However, the slow form of thrombin is reported to be relatively inactive toward fibrinogen and other procoagulant substrates, but the protease is capable of binding to TM and activating protein C with a normal catalytic efficiency (*4*).

Na^+ also plays a critical role in the structure and function of factor Xa (fXa), APC, and other coagulation proteases by binding to the same conserved 225-loop and modulating the catalytic activity of these proteases toward their specific

[†]The research discussed herein was supported by grants awarded by the National Heart, Lung, and Blood Institute of the National Institutes of Health (Grants No. HL 68571 and HL 62565).

*Corresponding author. Department of Biochemistry and Molecular Biology, St. Louis University School of Medicine, 1100 S. Grand Blvd., St. Louis, MO 63104. Phone: (314) 977-9240. Fax: (314) 977-9205. E-mail: rezaiear@slu.edu.

[1]Abbreviations: TM, thrombomodulin; EGF, epidermal growth factor; TM4−6, TM fragment containing EGF-like domains 4−6; fXa, activated factor X; Cys-67, Cys-82, Cys-217, Cys-224, thrombin mutants in which the indicated residues the chymotrypsin numbering system (*18*) have been replaced with a Cys; APC, activated protein C; AT, antithrombin; DTNB, 5,5′-dithiobis (2-nitrobenzoic acid); DTT, dithiothreitol; PEG, polyethylene glycol; BSA, bovine serum albumin.

Published on Web 07/29/2009

substrates (*20*−*23*). Mutagenesis and kinetic data have indicated that the Na^+-binding site and the primary S1 specificity site of these proteases are energetically linked (*24*). In addition to a linkage with the S1 subsite, it is also known that a thermodynamic linkage exists between the Na^+-binding and Ca^{2+}-binding sites of fXa and APC with the latter metal ion binding site being located on the 70−80-loop some ~30 Å away from the Na^+-binding site (*21*, *22*, *25*, *26*). This is the same loop that also binds Ca^{2+} in trypsin (*27*). The distinguishing Ca^{2+}-binding feature of this loop is that it has two acidic residues at positions 70 and 80, with both residues contributing to coordination of the divalent cation in this loop (*27*). However, the 70−80-loop of thrombin does not bind Ca^{2+} due to a nonconserved Lys at position 70 of thrombin salt-bridging with Glu-80, thereby stabilizing this loop independent of Ca^{2+} (*18*). Previously, we have shown that replacing the acidic residue at position 70 (or 80) of either APC or fXa with a Lys renders both proteases capable of functioning normally independent of Ca^{2+}, presumably due to the mutant Lys stabilizing this loop by a salt bridge, similar to the one that is observed in thrombin (*28*, *29*). The binding of TM4−6 to this loop of thrombin is thought to allosterically modulate the catalytic pocket of thrombin (*9*, *30*, *31*), though this hypothesis has not been supported by the X-ray crystal structure of the active-site inhibited thrombin−TM4−6 complex (*15*). Whether the inhibitor in the active-site of thrombin masks the TM dependent effect is not known. Recent studies have indicated that TM can also modulate the conformation of the 225-loop in the Na^+-binding defective mutants of thrombin (*12*, *32*, *33*), suggesting that the 70−80-loop may also be allosterically linked to the Na^+-binding loop of the protease. The extent to which TM modulates the catalytic pocket is not known, although there are several reports showing that TM alters the conformation of the extended substrate binding loops of the catalytic groove (*9*, *34*, *35*), thereby influencing the substrate specificity of thrombin in the anticoagulant pathway.

To further investigate these questions, we took a novel and structural-based mutagenesis approach and prepared two mutants of thrombin, in which the 70−80-loop in one and the 225-loop in the other were stabilized by an engineered disulfide bond between two adjacent residues Arg-67 and Ile-82 and Glu-217 and Lys-224 on the loops, respectively. Furthermore, we prepared an additional mutant in which Ser-195 of the protease was replaced with a Cys for direct labeling with a fluorescent probe. The characterization of these thrombin mutants in appropriate kinetic and direct binding assays provides critical insight into the nature of allostery in thrombin.

MATERIALS AND METHODS

Construction and Expression of Recombinant Proteins. Construction, expression, and purification of wild-type prethrombin-2 (prothrombin lacking the γ-carboxyglutamic acid and both kringle-1 and kringle-2 domains) in baby hamster kidney (BHK) cells using the pNUT-PL2 expression/purification vector system has been described (*36*). Prethrombin-2 mutants, in which two residues Arg-67 and Ile-82 in the first mutant and two residues Glu-217 and Lys-224 in the second mutant were replaced with Cys residues, were constructed by standard PCR mutagenesis methods and expressed in the same vector system as described (*36*). The same vector system was used to express and purify another prethrombin-2 mutant in which the catalytic residue Ser-195 was substituted with a Cys. Both wild-type and mutant proteins were activated with the taipan snake venom complex, and thrombin derivatives were purified on a Mono S column (Amersham Biosciences) as described (*36*). The active-site concentrations of enzymes were determined by stoichiometric titrations with calibrated concentrations of antithrombin (AT) in the absence or presence of heparin as described (*37*). The expression, purification, and characterization of the Lys-70 to Asp (K70D) mutant of thrombin (*38*), recombinant human protein C (*39*), and thrombomodulin fragment 4−6 (TM4−6) have been described (*39*).

Fluorescein-labeled Phe-Pro-Arg-ck (Fl-FPR) was purchased from Haematologic Technologies Inc. (Essex Junction, VT), and the fluorescent dye fluorescein-5-maleimide was purchased from Invitrogen (Carlsbad, CA). Normal pooled plasma was purchased from George King Bio-Medical, Inc. (Overland Park, KS). The unfractionated heparin, 5,5′-dithiobis (2-nitrobenzoic acid) (DTNB), dithiothreitol (DTT), and *Oxyuranus scutellatus scutellatus* venom (taipan venom) were purchased from Sigma (St. Louis, MO). The chromogenic substrates, Spectrozyme PCa (SpPCa) was purchased from American Diagnostica (Greenwich, CT), and S2238 was purchased from Kabi Pharmacia/Chromogenix (Franklin, OH).

Cleavage of Chromogenic Substrates. The steady-state kinetics of hydrolysis of S2238 (1−2000 μM) by thrombin derivatives (0.5−200 nM) was measured in 0.02 M Tris-HCl (pH 7.5), 0.2 to 1.0 M NaCl (or 0.2 to 1.0 M choline chloride) containing 0.1 mg/mL bovine serum albumin (BSA) and 0.1% polyethylene glycol (PEG) 8000 (TBS) at 405 nm at room temperature in a V_{max} Kinetic Microplate Reader (Molecular Devices, Menlo Park, CA) as described (*37*). The amidolytic activities of selected enzymes toward S2238 were also evaluated in the same TBS buffer system containing 1 mM DTT. The dependence of initial rates of substrate cleavage on the substrate concentration was fit by nonlinear regression to the Michaelis−Menten equation to obtain K_m and k_{cat}.

Clotting Activity. The clotting activities of thrombin derivatives toward normal plasma were compared using an ST4 Biocoagulometer (Diagnostica/Stago, Asnieres, France). Plasma clotting was initiated by the addition of 100 μL of thrombin (10−100 nM final concentrations) in TBS to 100 μL of citrated human plasma at 37 °C.

Binding to TM4−*6*. The affinity of exosite-1 of thrombin mutants for interaction with TM was evaluated by the competitive effects of mutants on the TM4−6-mediated protein C activation by wild-type thrombin as described (*39*). Briefly, the rate of activation of human protein C (1 μM) by thrombin (1 nM) in complex with TM4−6 (5 nM) was monitored in the presence of increasing concentrations of either Cys-67/Cys-82 or Cys-217/Cys-224 thrombins in 0.02 M Tris-HCl (pH 7.5), 0.1 M NaCl, 0.1 mg/mL BSA, and 0.1% PEG 8000 (TBS) containing 2.5 mM Ca^{2+}. The catalytically inactive S195A thrombin, which has normal affinity for TM, was used as a control. Following 15−30 min of activation at room temperature, antithrombin (750 nM in complex with 1 μM heparin) was added to inhibit the thrombin activity, and the concentration of APC generated in each reaction was measured by an amidolytic activity assay using SpPCa. To simplify comparisons of the competitive effects of thrombin mutants on the activation reaction, all kinetic data were normalized to maximal APC generation in the absence of the competitors. The dissociation constants (K_D) for the interaction of TM4−6 with exosite-1 of thrombin mutants were calculated using a competitive binding equation as described (*40*).

Binding to Na^+. The affinity of Na^+ for interaction with thrombin derivatives was evaluated by the ability of the metal ion to increase the intrinsic protein fluorescence upon binding using an Aminco-Bowman series 2 Spectrophotometer (Spectronic Unicam, Rochester, NY) as described (*41*, *42*). Briefly, thrombin derivatives were dialyzed into 5 mM Tris-HCl (pH 8.0) and 0.1% PEG 8000 buffer, and then diluted to 50 nM in two 500 μL cuvettes containing either 0.8 M NaCl or 0.8 M choline chloride. The Na^+ concentration of the thrombin sample in the choline chloride cuvette was varied from 0 to 300 mM by successively removing 5−10 μL aliquots of the thrombin solution and replacing them with an equal volume of the thrombin solution in NaCl. The protein fluorescence after each addition was monitored at 10 °C at excitation and emission wavelengths of 295 and 333 nm, respectively. The saturable changes in the intrinsic protein fluorescence of each derivative upon binding to Na^+ were computer-fit to a hyperbolic equation to obtain equilibrium dissociation constants (K_D) for the metal ion.

Binding to Heparin. The affinities of thrombin derivatives for interaction with heparin were evaluated by monitoring the enhancement in the intrinsic fluorescence of proteins upon binding heparin. Briefly, small aliquots of heparin were successively added to 100 nM thrombin in 0.02 M Tris-HCl (pH 7.5), 0.1 M NaCl, and 0.1% PEG 8000 buffer (TBS), and the change in the protein fluorescence was recorded at 25 °C at excitation and emission wavelengths of 292 and 333 nm, respectively. The changes in the intrinsic fluorescence of the thrombin derivatives as a function of [heparin] were best fit to Langmuir binding isotherm using the equation for two ligand binding sites.

Binding to Heparin-Sepharose. Wild-type and mutant thrombins (5 μg) in TBS were applied on a 1.0-mL heparin-Sepharose column pre-equilibrated with the same buffer as described (*43*). The column was washed with 2 mL of TBS followed by elution with a step gradient of 0.1−0.6 M NaCl using increments of 10−20 mM salt. At each step, 0.5 mL of buffer was used to elute the bound enzymes from the column. To determine the elution positions, a 25 μL aliquot from each fraction was transferred to a 96-well plate, and their amidolytic activities toward the chromogenic substrate S2238 (100 μM) were determined.

Fluorescent Labeling. Thrombin (~0.5 mg) in TBS (0.1 M NaCl and 0.02 M Tris-HCl at pH 7.5) was incubated with 10-fold molar excess of Fl-FPR-chloromethylketone for 2 h at room temperature in the dark. The extent of active-site labeling was monitored by the loss of the enzymatic activity using S2238. Incubation was continued until more than 99.9% of the activity was inhibited. For the Cys-195 labeling of thrombin-Cys-195, the same amount of the mutant protease was incubated with fluorescein-5-malimide (200 μM) in TBS containing 25 μM dithiothreitol to ensure the reduction of the free cysteine for 2 h at room temperature in the dark. This level of reducing agent did not influence the activity of thrombin. The free inhibitor or dye was separated from the labeled proteins by gel filtration on the PD-10 column followed by their extensive dialysis in TBS at 4 °C in the dark. The extent of fluorescence labeling for all proteins was determined as described by Bock (*44*). An extinction coefficient of 84,000 M^{-1} cm^{-1} at 498 nm was used to calculate the fluorescein concentration, and the ratio $\varepsilon_{280\ nm}/\varepsilon_{498\ nm} = 0.19$ was used to correct for the contribution of the dye to 280-nm absorbance of the proteins as described (*44*). The average number of dyes per protein was determined to be ~0.6 for the Fl-FPR-labeled and ~0.5 for the Cys-195 labeled thrombins.

Fluorescence Measurements. The affinities of the fluorescein labeled thrombin derivatives for interaction with Na^+, TM4−6, and heparin were evaluated by changes in the fluorescence of the proteins upon their interaction with each ligand. Briefly, small aliquots of each ligand was added to 50 nM of the labeled proteins in TBS, and changes in the fluorescence intensities were recorded at 25 °C at excitation and emission wavelengths of 493 and 521 nm, respectively. In the case of Na^+ binding to labeled proteins, the proteins were diluted to either NaCl containing or choline chloride containing buffer in order to keep the ionic strength constant as described above. The nonlinear regression analysis of data yielded equilibrium dissociation constants for each ligand as described (*45*).

Molecular Modeling. Modeling of an engineered disulfide bond in a mutant protein requires software capable of introducing a new disulfide bond into an existing structure. We used VMD (*46*) and NAMD (*47*) programs to introduce new disulfide bonds by patching the structural files (.psf) of mutants, followed by their energy minimization. The procedure of patching converts the two engineered free Cys residues to a disulfide link. The starting coordinates for our models were taken from the high-resolution (1.47 Å) crystallographic structure of thrombin (PDB code 2ZFF). The structure was solvated in the TIP3P model water (*48*) to produce a 10 Å thick water shell around the protein. To maintain electrical neutrality, sodium ions were added to the system. The minimization script generated by the VMD program instructed NAMD to do 1000 steps of conjugate-gradient energy minimization to remove steric clashes within the guessed geometry of mutants. The minimization was carried out using NAMD2 (*47*, *49*, *50*) with the CHARMM27 force field (*51*). The resulting structures were analyzed using VMD (*46*) and UCSF Chimera (*52*) software.

RESULTS

Expression, Activation, and Purification of Thrombin Derivatives. The zymogen forms of both wild-type and mutant thrombins were expressed as prethrombin-2 zymogens in the pNUT-PL2 expression/purification vector system in BHK cells and purified to homogeneity as described (*36*, *37*). All zymogen mutants were converted to thrombin by the taipan venom complex and analyzed by sodium dodecyl sulfate−polyacrylamide gel electrophoresis (SDS−PAGE) under nonreducing conditions. The thrombin mutants migrated as monomeric molecules with similar expected apparent molecular masses of ~37 kDa, suggesting that the engineered Cys residues in both Cys-67/Cys-82 and Cys-217/Cys-224 mutants have likely formed a disulfide bond in each construct (data not shown). Titration of mutants with DTNB did not also detect a free Cys. The Cys-195 mutant of thrombin also migrated primarily as a monomeric molecule, suggesting that this residue is shielded within the active-site groove and, thus, is not capable of interacting intermolecularly to form dimers or higher molecular weight aggregates. The Cys-195 mutant was labeled with fluorescein-5-malimide and, following extensive dialysis against TBS, was frozen in small aliquots at −80 °C until use.

Amidolytic and Proteolytic Activity. The concentration dependence of the amidolytic activity of wild-type, Cys-67/Cys-82, and Cys-217/Cys-224 thrombins toward the chromogenic substrate S2238 under different conditions is presented in Figures 1 and 2. The Cys-67/Cys-82 mutant of thrombin exhibited essentially normal amidolytic activity in the Tris-HCl

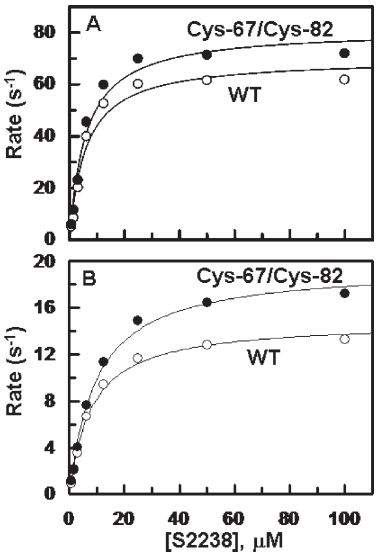

FIGURE 1: Comparison of the amidolytic activity of wild-type and Cys-67/Cys-82 thrombins. (A) The amidolytic activity of thrombin (○) and thrombin-Cys-67/Cys-82 (●) (1 nM each) toward increasing concentrations of S2238 was analyzed in 0.02 M Tris-HCl (pH 7.5) containing 0.2 M NaCl, 0.1 mg/mL BSA, and 0.1% PEG 8000 as described in Materials and Methods. (B) The same as panel A except that 0.2 M choline chloride replaced NaCl in the reaction buffer. Solid lines are nonlinear regression fits of the average kinetic data from three independent measurements to the Michaelis−Menten equation. The K_m and k_{cat} values are presented in Table 1.

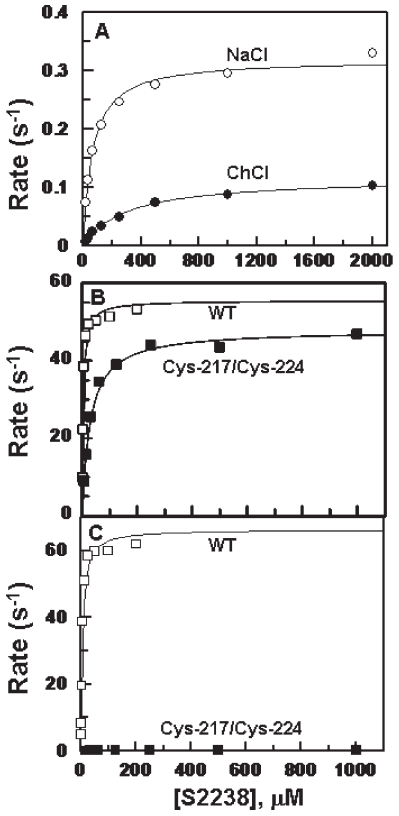

FIGURE 2: Comparison of the amidolytic activity of Cys-217/Cys-224 thrombin in NaCl and choline chloride. (A) The amidolytic activity of Cys-217/Cys-224 (100−200 nM) toward increasing concentrations of S2238 was analyzed in 0.02 M Tris-HCl (pH 7.5), 0.1 mg/mL BSA, and 0.1% PEG 8000 containing either 0.2 NaCl (○) or 0.2 M choline chloride (●). (B) The amidolytic activity of wild-type thrombin (□) or Cys-217/Cys-224 (■) (0.5−1 nM) toward increasing concentrations of S2238 was analyzed in 0.02 M Tris-HCl (pH 7.5), 1 M NaCl, 0.1 mg/mL BSA, and 0.1% PEG 8000 containing 1 mM DTT as described in Materials and Methods. (C) The same as panel B with the exception that the amidolytic activities were monitored in the absence of DTT. Solid lines are nonlinear regression fits of the average kinetic data from three independent measurements to the Michaelis−Menten equation. The K_m and k_{cat} values are presented in Table 1.

buffer containing either 0.2 M NaCl (Figure 1, panel A) or 0.2 M choline chloride (Figure 1, panel B), suggesting that a disulfide bond between Cys-67 and Cys-82 may have formed and that the mutagenesis has no adverse effect on the folding or the reactivity of the catalytic triad and the P3−P1 binding pocket of the mutant protease. However, unlike this mutant, the amidolytic activity of the Cys-217/Cys-224 mutant was dramatically impaired (Figure 2, panel A). The decline in the amidolytic activity of this mutant was due to an ~10−30-fold elevation in K_m for S2238 and ~140−230-fold decrease in the k_{cat} for hydrolysis of this chromogenic substrate in TBS containing either 0.2 M NaCl or 0.2 M choline chloride (Figure 2 and Table 1). Interestingly, most of the amidolytic activity of this mutant was restored if the disulfide bonds of thrombin were reduced by 1 mM DTT (Figure 2). This concentration of DTT was determined to be optimal for restoring the k_{cat} for the hydrolysis of S2238 by Cys-217/Cys-224 to a normal level without having a significant effect on the activity of wild-type thrombin (Figure 2, panel B and Table 1). Only the K_m of this mutant for the substrate remained elevated (~15-fold in 0.2 M NaCl and ~7-fold in 1.0 M NaCl) in DTT (Table 1), which suggests that the stabilization of the Na^+-loop by a disulfide bond is responsible for the dramatic decline in the cleavage rate of the chromogenic substrate by the Cys-217/Cys-224 mutant.

The clotting activities of both thrombin mutants were also dramatically impaired. Thus, in a normal plasma clotting assay in which 10 nM wild-type thrombin yielded a clotting time of 19 s, neither Cys-67/Cys-82 nor Cys-217/Cys-224 clotted plasma up to 360 s of monitoring under these conditions (Table 1). While 100 nM of Cys-67/Cys-82 yielded a clotting time of 238 s, again no clotting activity for the Cys-217/Cys-224 was observed under these conditions up to 360 s of monitoring, suggesting that the defect in the clotting activity of the latter mutant is much more dramatic than that of the former mutant (Table 1).

The protein C activation properties of both thrombin mutants were also dramatically impaired since no TM-dependent protein C activation could be detected for either mutant. To determine whether the defects in the variants were due to the loss of exosite-1 binding, their ability to function as competitive inhibitors of TM4−6-dependent protein C activation by wild-type thrombin was evaluated. As shown in Figure 3, the Ser-195 to Ala (S195A) substitution mutant of thrombin effectively inhibited the TM4−6-dependent activation of protein C by wild-type thrombin with a dissociation constant of 9.0 ± 1.5 nM that is similar to $K_{d(app)}$ for the interaction of the TM fragment with thrombin in similar previous kinetic studies (*53*). However, Cys-67/Cys-82 had no competitive effect on the TM4−6-dependent activation of protein C by thrombin and the competitive effect of Cys-217/Cys-224 was drastically reduced so that a $K_{d(app)}$ of ~200 nM was estimated for the interaction of this mutant with TM4−6, suggesting ~20-fold impairment for the interaction of the mutant with the cofactor fragment (Figure 3). The dramatic impairment in the interaction of TM4−6 with Cys-67/Cys-82 was expected and is consistent with previous studies assigning an essential role for Arg-67 of thrombin for interaction with exosite-1 specific

Table 1: Amidolytic and Plasma Clotting Activities of Thrombin Derivatives[a]

	WT		Cys-67/Cys-82		Cys-217/Cys-224	
S2238	K_m (μM)	k_{cat} (s^{-1})	K_m (μM)	k_{cat} (s^{-1})	K_m (μM)	k_{cat}(s^{-1})
NaCl (0.2 M)	5.9 ± 0.3	75.0 ± 6.4	5.9 ± 0.2	84.4 ± 5.4	62.0 ± 6.4	0.32 ± 0.007
ChCl (0.2)	8.8 ± 0.8	15.8 ± 1.4	10.6 ± 0.6	21.2 ± 1.7	298 ± 28	0.11 ± 0.004
NaCl (0.2 M + DTT)	6.4 ± 1.6	46.6 ± 2.7	ND	ND	95.6 ± 2.9	41.2 ± 1.1
NaCl (1.0 M + DTT)	3.9 ± 0.8	55.5 ± 2.3	ND	ND	28.7 ± 2.3	47.9 ± 0.9
plasma clotting	sec		sec		sec	
thrombin (10 nM)	19		> 360		> 360	
thrombin (100 nM)	ND		238		> 360	

[a] The kinetic constants were determined from the steady-state kinetics of hydrolysis of S2238 (2-2000 μM) by each enzyme (0.5−200 nM) in Tris-HCl (pH 7.5) containing 0.2−1 M of either NaCl or choline chloride (ChCl) in the absence or presence of 1 mM DTT at room temperature as described in Materials and Methods. All values are the average of at least 3 measurements ± S.E. Data are derived from Figures 1 and 2. The one stage plasma clotting time was measured using normal plasma as described in Materials and Methods.

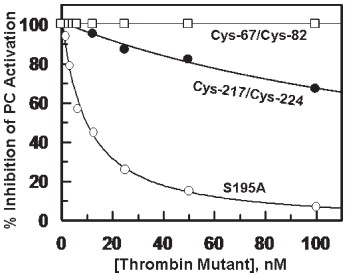

FIGURE 3: Competitive effects of thrombin mutants on the TM4−6-mediated protein C activation by thrombin. The TM4−6 (5 nM) mediated activation of human protein C (PC, 1 μM) by wild-type thrombin (1 nM) was monitored in TBS containing 2.5 mM Ca^{2+} at room temperature in the presence of increasing concentrations of thrombin-S195A (○), thrombin-Cys-67/Cys-82 (□), or thrombin-Cys-217/Cys-224 (●) as described in Materials and Methods. Following the neutralization of the thrombin activity by antithrombin, the rate of activated protein C generation and its extent of inhibition by the competitors were measured by an amidolytic activity using Spectrozyme PCa. The solid lines are nonlinear regression fits of kinetic data from three independent measurements to a competitive binding equation.

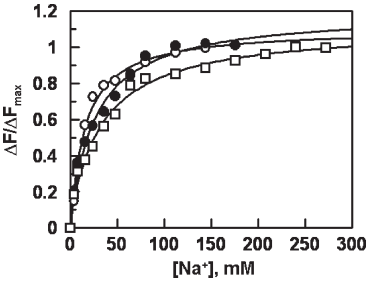

FIGURE 4: Na^+ binding to thrombin derivatives. The Na^+-binding curves were generated from the saturable enhancement in the intrinsic fluorescence of thrombin derivatives as a function of the cation concentration. The solid lines are nonlinear regression fits of fluorescence data from three independent measurements to a hyperbolic equation which yielded K_D values of 14 mM for wild-type thrombin (○), 27 mM for Cys-67/Cys-82 (●), and 34 mM for Cys-217/Cys-224 (□) for the metal ion.

ligands (*35*, *54*); however, the 20-fold increase in the dissociation constant for the interaction of TM4−6 with Cys-217/Cys-224 was surprising. This result clearly suggests that the stabilization of the Na^+-binding loop by a disulfide bond has a dramatic effect on the conformation of exosite-1.

Interaction with Na^+. The equilibrium dissociation constants for interaction of thrombin derivatives with Na^+ were determined from the Na^+-mediated enhancement in the intrinsic fluorescence of thrombin upon interaction with the metal ion as has been previously described (*41*). Wild-type thrombin bound Na^+ with a K_D of 14 ± 3 mM, which is consistent with the literature under essentially identical experimental conditions (*41*). K_D values for the interaction of Na^+ with Cys-67/Cys-82 (27 ± 4 mM) and Cys-217/Cys-224 (34 ± 4 mM) were elevated 2- and 2.5-fold, respectively (Figure 4). A similar 2-fold higher apparent dissociation constant ($K_{d(app)}$) for Cys-67/Cys-82 thrombin was obtained using an amidolytic activity assay with S2238 as the substrate; however, the $K_{d(app)}$ for the interaction of Cys217/Cys-224 thrombin was elevated > 10-fold (data not shown). Nevertheless, Na^+ promoted the amidolytic activity of the mutants to a similar extent as in wild-type thrombin (~10-fold), supporting the direct binding data that Na^+ can interact with mutants, although with lower affinities. We have previously reported the expression and characterization of a Lys-70 to Asp (K70D) mutant of thrombin (*38*). We evaluated the affinity of Na^+ for interaction with K70D thrombin in the current study and discovered that there is no enhancement in the intrinsic fluorescence of this mutant upon interaction with Na^+ (data not shown). Taken together, these results further support the hypothesis that the conformations of the 70−80-loop of exosite-1 and Na^+-binding loop are allosterically linked. This hypothesis is consistent with the literature (*12*). Furthermore, the modest elevation in the K_D of Cys-217/Cys-224 thrombin for interaction with Na^+ in the direct binding assay suggests that the conformation of the 225-loop is not drastically changed by the new disulfide bond (see the molecular modeling results below). Thus, it appears that the engineered disulfide bond between Cys-217 and Cys-224 can fulfill the function of a salt bridge, which serves to orient the carbonyl oxygen atoms of Arg-221a and Lys-224 to appropriate positions in order to allow them to participate in the coordination of Na^+ (*20*, *41*).

Interaction with Heparin. To evaluate the conformational state of exosite-2 of thrombin derivatives, the ability of the mutant proteases to interact with heparin was evaluated. Both Cys-67/Cys-82 and Cys-217/Cys-224 bound heparin with an affinity profile similar to that of the wild-type thrombin, as monitored from the analysis of changes in the intrinsic protein fluorescence upon interaction with heparin (Figure 5A). The

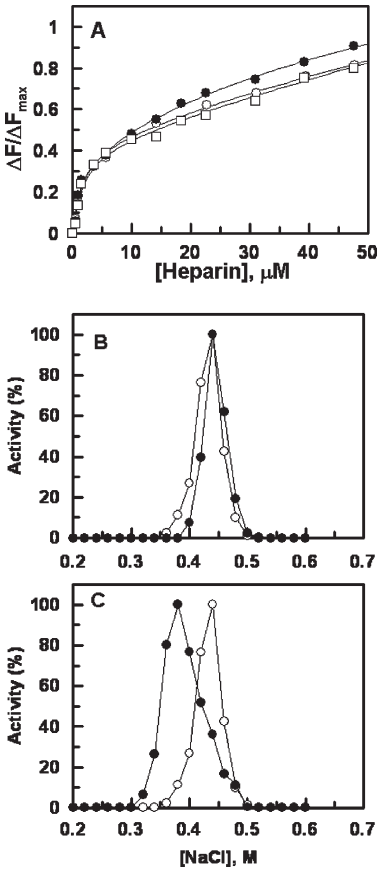

FIGURE 5: Binding of heparin to thrombin derivatives. (A) The heparin-binding curves were generated from the enhancement in the intrinsic fluorescence of thrombin derivatives as a function of heparin concentration as described in Materials and Methods. The solid lines are nonlinear regression fits of fluorescence data from three independent measurements to the Langmuir binding isotherm using the equation for two ligand binding sites which yielded a K_D value of $\sim$1−1.5 μM for all thrombin derivatives for the first binding site and a much higher K_D value of $>$200 μM for the second site. The symbols are as follows: (○) wild-type thrombin, (●) Cys-67/Cys-82, and (□) Cys-217/Cys-224. (B) NaCl gradient elution profiles of wild-type thrombin (○) and Cys-67/Cys-82 (●) from heparin-Sepharose. (C) NaCl gradient elution profiles of wild-type thrombin (○) and prethrombin-2 (●) from heparin-Sepharose.

titration data fit the best to a binding equation describing two ligand-binding sites. This is likely due to higher concentrations of heparin binding to the anion-binding exosite-1 of thrombin. The K_D for the first binding site, which represents heparin binding to exosite-2, was $\sim$1−1.5 μM for all three proteins, and that of the second-binding site, which was not fully saturable, is estimated to be higher than 200 μM, supporting the hypothesis that heparin nonspecifically binds to exosite-1 of thrombin (Figure 5A). These results are consistent with those of a previous study which also observed a second weaker binding site on thrombin for heparin (*55*). Both wild type and Cys-67/Cys-82 eluted from the heparin-Sepharose column at an identical NaCl concentration of 0.45 M, further supporting an identical affinity for heparin by both proteins (Figure 5B). These results suggest that exosite-2 is not conformationally linked to either exosite-1 or the 225-loop in thrombin. It is known that exosite-1 of thrombin exists as pro-exosite-1 in prothrombin and prethrombin-2 having $\sim$100-fold lower affinity for the exosite-1-specific ligands TM4−6 and the hirudin C-terminal peptide (*40*, *56*). However, as shown in Figure 5C, heparin can bind to exosite-2 of thrombin in the

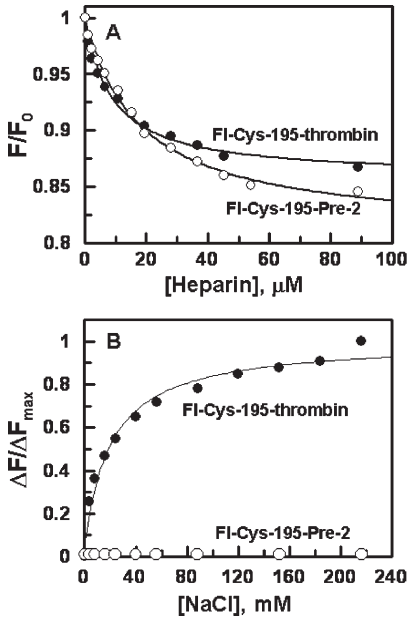

FIGURE 6: Binding of heparin and Na^+ to fluorescein labeled thrombin-Cys-195 and prethrombin-Cys-195. (A) The heparin-binding curves were generated from the changes in the fluorescence of fluorescein attached to Cys-195 of either thrombin (●) or prethrombin-2 (○) as a function of heparin concentration as described in Materials and Methods. The solid lines are nonlinear regression fits of fluorescence data from three independent measurements yielding K_D values of 9 ± 1 μM and 18 ± 2 μM for thrombin and prethrombin-2, respectively. (B) The Na^+-binding curves were generated from the changes in the fluorescence of fluorescein attached to Cys-195 of either thrombin (●) or prethrombin-2 (○) as a function of Na^+ concentration yielding a K_D value of 17 ± 3 mM for the metal ion interaction with thrombin-Cys-195. Na^+ did not bind to prethrombin-2-Cys-195.

zymogen prethrombin-2 with only a slightly lower affinity, thus eluting from the heparin-Sepharose column at the NaCl concentration of 0.4 M. Further studies with the fluorescein labeled thrombin-Cys-195 and prethrombin-2-Cys-195 revealed that K_D for the interaction of heparin with exosite-2 of the prethrombin-2 is nearly comparable to that of wild-type thrombin (Figure 6A). With the fluorescein-labeled proteins, monophasic binding curves were observed (Figure 6A). The basis for discrepancy between the heparin-binding curves of intrinsic and extrinsic fluorescence measurements is not known, but it could arise from inherent differences in methodologies since the former approach is reporting changes in the environment of several Trp residues (a total of nine) which are distributed over the entire structure of thrombin (*57*), whereas the latter approach is reporting the change in the environment of a single fluorophore dye attached to the active-site pocket of thrombin. Unlike a normal interaction of prethrombin-2 with heparin, the fluorescein-labeled Cys-195 zymogen did not bind Na^+, suggesting that the activation of the zymogen is associated with a conformational change in the Na^+-binding loop but not in exosite-2 of thrombin (Figure 6B).

Linkage to Active Site. To investigate whether the conformations of the Na^+-binding 225-loop and exosite-1 of thrombin are linked to the catalytic pocket, we prepared a fluorescein-labeled Cys-195 mutant of thrombin and monitored the change in the fluorescent of the catalytic residues upon interaction with either Na^+ or TM4−6. As shown in Figure 6B, the binding of Na^+ to thrombin enhanced the intensity of the fluorophore bound to the catalytic residue of thrombin in a concentration

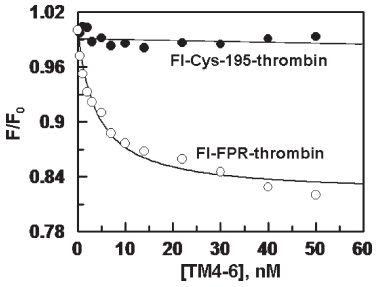

FIGURE 7: Binding of TM4−6 to fluorescein labeled thrombins. The TM4−6-binding curves were generated from the changes in the fluorescence of fluorescein attached to either Cys-195 thrombin (●) or Fl-FPR-inhibited thrombin (○) as a function of TM4−6 concentration as described in Materials and Methods. The solid line for Fl-FPR-thrombin is nonlinear regression fits of fluorescence data from three independent measurements yielding K_D of 3.5 ± 0.5 nM for TM4−6 binding to the active-site inhibited thrombin.

dependent manner with a K_D value of 17 ± 3 mM, which is similar to the same value (14 ± 3 mM) obtained above for wild-type thrombin in Figure 4 by monitoring the intrinsic fluorescence of the protein. However, the titration of the fluorescein-labeled thrombin-Cys-195 with increasing concentrations of TM4−6 was not associated with any change in the fluorescence intensity of the dye in the active-site pocket of thrombin (Figure 7). Nevertheless, the binding of TM4−6 to exosite-1 of thrombin, inhibited by the fluorescein tethered FPR, was associated with a robust change in the catalytic groove of the active-site inhibited thrombin with a K_D of 3.5 ± 0.5 nM (Figure 7), as has been previously demonstrated by others (*34*). These results suggest that the catalytic residue Ser-195 is energetically linked to the Na^+-binding loop of thrombin; however, it is not the catalytic residue, but the extended substrate binding pocket of thrombin that may be allosterically modulated by TM4−6 binding to exosite-1 of thrombin. The possibility that TM4−6 may alter the conformation of the catalytic residue in the absence of Na^+ was not investigated.

Molecular Modeling. Modeling of thrombin mutants suggested that the loops can adopt newly formed disulfide bonds without considerable changes in their conformations (data not shown). The distances between the SG atoms of engineered Cys residues involved in disulfide bond formation in the mutants before minimizations were more than 3 Å in both cases, which are too distant to allow S−S bond formation in these structures. Energy minimization combined with the patching described in Materials and Methods placed Cys SG atoms at distances of 2.003 Å and 2.030 Å for Cys-67/Cys-82 and Cys-217/Cys-224 mutants, respectively. This is an average length of an S−S bond, suggesting that these mutants can readily accommodate newly formed disulfide bonds. In order to characterize the conformational changes due to mutations, we measured root-mean-square deviations (rmsd) for the frames in the trajectories saved during minimizations. The RMSDs for the whole molecule measured by comparison of the first frame with the last frame (end of minimization) were 0.542 Å, 0.465 Å, and 0.549 Å for wild type, Cys-67/Cys-82 ,and Cys-217/Cys-224, respectively. The RMSDs for either the 70−80-loop or the Na^+-binding loop did not change during minimization, suggesting that the overall conformation of the molecules in general or the conformation of the loops under study in particular may have been minimally affected by the newly introduced disulfide bonds. A comparison of the salt bridges that potentially form in wild-type and mutant thrombins showed that all three structures share 23 salt bridges. However, mutated residues Glu-217 and Lys-224 form a salt bridge in the wild-type thrombin (*20*, *33*, *58*); therefore, this bridge is lost in the Na^+-loop mutant. Nevertheless, the newly formed disulfide bond between these residues could substitute for the salt bridge, possibly explaining the basis for the ability of the 225-loop to bind Na^+ in the mutant. Because of obvious differences in the nature of disulfide bonds and salt bridges, it is expected that the mutagenesis will restrict the plasticity of mutants; however, we did not simulate long-range communications and solely relied on the experimental data to provide support for our hypothesis.

DISCUSSION

The activity of the vitamin K-dependent coagulation proteases is allosterically modulated by the monovalent cation Na^+ binding to the 225-loop and the divalent cation Ca^{2+} binding to the 70−80-loop on the catalytic domain of these proteases (*12*, *28*, *29*, *41*). The presence of a conserved Tyr at position 225 (*23*) and two acidic Asp or Glu at both positions 70 and 80 (*28*, *29*) of these proteases is a signature for their ability to interact with Na^+ and Ca^{2+}, respectively. These two metal ion binding sites are located ~30 Å away from each other on two opposite sides of the catalytic pockets (*12*, *25*, *26*). In the case of both fXa and APC, which contain both of these structural features, we demonstrated that there is an allosteric linkage between the two metal ion binding sites, thus altering the affinity of one site for its specific cation by a mutagenesis approach led to a similar alteration in the affinity of the other site for its specific metal ion (*21*, *22*). In the case of thrombin, the 70−80-loop, which is centered on exosite-1 of the protease, is stabilized by a salt bridge between Lys-70 and Glu-80, providing the structural basis for thrombin functioning independent of Ca^{2+} (*13*, *18*). To investigate whether or not the conformation of exosite-1 is energetically linked to other functionally critical sites of the protease (i.e., the Na^+-binding site, exosite-2, and active-site), we took a novel mutagenesis approach and stabilized either the 70−80-loop or the 225-loop of thrombin by engineered disulfide bonds in separate constructs. Thus, in the first construct, we replaced the native residues Arg-67 and Ile-82 of thrombin with Cys residues. The rationale for this approach is based on our previous finding with APC that an ionic interaction between Arg-67 and Asp-82 of protein C modulates the Ca^{2+}-dependence of zymogen activation by thrombin in the absence and presence of TM (*35*). The examination of the crystal structure of the protease domain of APC suggested that these two residues are located within a salt-bridging distance on two antiparallel β strands which form the 70−80-loop of the molecule (*26*). Interestingly, the substitutions of these residues with two Cys resulted in a mutant, the loop of which was stabilized by a disulfide bond and functioned normally independent of Ca^{2+} (*35*). Furthermore, the stabilization of the 70−80-loop by a disulfide bond trapped the 225-loop of APC in the high-affinity Na^+ conformation suggesting that the two sites are energetically linked (*35*). Asp-82 of APC is not conserved in thrombin. However, noting that both Arg-67 and Ile-82 of thrombin are only ~3 Å apart in the structure of thrombin and that both occupy the same three-dimensional positions as those in APC, we hypothesized that a similar disulfide bond may form between the engineered Cys residues in thrombin. Indeed, the observations that the Cys-67/Cys-82 thrombin migrated in a monomeric form and exhibited essentially identical amidolytic activity are consistent with the proposal that a disulfide bond has formed between the two Cys

mutants. The molecular modeling data is also consistent with this hypothesis.

The rationale for the construction of the Cys-217/Cys-224 mutant was also based on the thrombin structural data showing that a salt bridge between Glu-217 and Lys-224 is required in order to orient the carbonyl oxygen atoms of both Arg-221a and Lys-224 to appropriate positions so that they can participate in the coordination of Na^+ in the 225-loop (*20*, *58*). Thus, we hypothesized that replacing these residues with Cys may result in the formation of a disulfide bond, thus mimicking the salt bridge and trapping thrombin in Na^+-stabilized fast conformation. The observation that this mutant also migrated as a monomeric molecule on the nonreducing SDS−PAGE, and bound Na^+ is consistent with the hypothesis that a proper disulfide bond may have formed between the engineered residues. Nevertheless, the observation that this mutant was essentially inactive was surprising. The salt bridge between the two residues Glu-217 and Lys-224 must be in a dynamic state allowing the information from Na^+ binding to the 225-loop to be communicated to allosteric sites in thrombin, and this process has been eliminated in the disulfide-stabilized Cys-217/Cys-224 thrombin. Both the molecular modeling and biochemical data suggest that the engineered disulfide bond meets the structural requirements for reorienting the O carbonyl atoms of residues 224 and Arg-221a so that this loop can coordinate a Na^+ ion. However, it appears that the stabilization of this loop locks it in a rigid and nonflexible conformation, thereby preventing this loop from transmitting Na^+-mediated information to the active site and exosite-1 of thrombin. The observation that the elimination of this disulfide bond by DTT completely restored the k_{cat} of the mutant protease toward S2238 is also consistent with this hypothesis. It should be, however, noted that there is another disulfide bond near the two engineered Cys-217 and Cys-224 residues (between Cys-191 and Cys-220); it is also possible that the mutant residues have formed new alternative disulfide bonds with these residues (i.e., Cys-217 with Cys-191 and Cys-224 with Cys-220). While in the absence of a crystal structure, this possibility cannot be ruled out; nevertheless, the result of a previous study has demonstrated that the disulfide bond between Cys-191 and Cys-220 is required for the interaction of Na^+ with thrombin (*59*). The same previous study has further shown that a thrombin mutant lacking the 191−220 disulfide bond does not undergo Na^+-mediated fluorescence changes (*59*). The observation that Cys-217/Cys-224 mutant binds Na^+ with near normal affinity and undergoes normal Na^+- and heparin-induced intrinsic fluorescence changes strongly argues against the alternative mis-matched disulfide bonding possibility in the mutant protein. Nevertheless, the crystal structure of this mutant needs to be resolved to confirm the validity of this hypothesis.

The observation that the amidolytic activity of thrombin Cys-67/Cys-82 was not adversely affected by the engineered disulfide bond does not support the existence of an allosteric linkage between exosite-1 and catalytic residues of thrombin. This hypothesis is also consistent with the binding data where TM4−6 did not alter the intensity of the fluorescein dye attached directly to Cys-195 in the mutant thrombin. Nevertheless, in agreement with previous results (*34*), TM4−6 induced a conformational change in the active-site groove of thrombin inhibited by the fluorescein labeled FPR-ck, suggesting that TM4−6 induces a conformational change in the extended substrate binding pocket of thrombin. The structural data predicts that this strategy of active-site labeling would position the fluorescein dye (attached to the P3 Phe) ~15 Å away from Ser-195 in the active-site groove of thrombin and other coagulation proteases (*18*, *60*). In the case of factors IXa and Xa, based on the binding studies using Fl-FPR-labeled proteins, it has been hypothesized that the cofactor binding sites of both proteases are conformationally coupled to a region of the active-site pocket that is located some 15 Å from Ser-195 (*60*). Thus, it appears that TM induces conformational changes in the extended substrate binding pocket of thrombin, but the catalytic residue of thrombin may not be modulated by TM binding to the exosite-1 of thrombin. This hypothesis is also consistent with structural data showing that the catalytic residues of the active-site pocket of the FPR-inhibited thrombin in both unbound and TM4−6-bound forms have essentially identical conformations (*15*). However, a recent crystal structure of thrombin which did not have a tripeptidyl inhibitor in the active-site revealed that the occupancy of exosite-1 by the hirudin-like peptide derived from the C-terminal domain of protease-activated receptor-3 allosterically modulates the conformation of the 60-loop and shifts the position of Trp-60d in this loop ~10 Å, thereby widening the access to the active site of the protease (*61*). Thus, similar to the cofactor function of factor Va in the prothrombinase complex, TM may not alter the conformations of the catalytic residues of thrombin but rather those of the extended substrate binding sites surrounding the catalytic groove of the protease (*9*, *30*, *31*). This is likely to be the primary mechanism by which TM promotes the catalytic activity of thrombin toward protein C in the anticoagulant pathway (*6*).

Finally, the observation that the thrombin derivatives interacted with heparin with essentially identical affinities does not support the conclusion of a previous study that exosite-1 and exosite-2 of thrombin are energetically linked (*62*), but rather our results are consistent with another study reporting no linkage between these two cofactor binding sites in thrombin (*63*). Furthermore, the observation that prethrombin-2 did not bind Na^+ suggests that, similar to exosite-1 (*56*), the 225-loop undergoes a dramatic conformational change upon activation of the zymogen. However, the near normal affinity of prethrombin-2 for heparin suggests that exosite-2 is expressed in zymogen form, although this site is not available for interaction with heparin in prothrombin because of fragment 2 binding to this site of the molecule (*64*).

ACKNOWLEDGMENT

We thank Audrey Rezaie for proofreading the manuscript.

REFERENCES

1. Mann, K. G., Jenny, R. J., and Krishnaswamy, S. (1988) Cofactor proteins in the assembly and expression of blood clotting enzyme complexes. *Annu. Rev. Biochem. 57*, 915–956.
2. Furie, B., and Furie, B. C. (1988) The molecular basis of blood coagulation. *Cell 53*, 505–518.
3. Davie, E. W., Fujikawa, K, and Kisiel, W. (1991) The coagulation cascade: Initiation, maintenance and regulation. *Biochemistry 30*, 10363–10370.
4. Dang, Q. D., Vindigni, A., and Di Cera, E. (1995) An allosteric switch controls the procoagulant and anticoagulant activities of thrombin. *Proc. Natl. Acad. Sci. U.S.A. 92*, 5977–5981.
5. Lane, D. A., Philippou, H., and Huntington, J. A. (2005) Directing thrombin. *Blood 106*, 2605–2612.
6. Esmon, C. T. (1993) Molecular events that control the protein C anticoagulant pathway. *Thromb. Haemost. 70*, 1–5.
7. Tsiang, M., Lentz, S., and Sadler, J. E. (1992) Functional domains of membrane-bound human thrombomodulin. EGF-like domains four to six and the serine/threonine-rich domain are required for cofactor activity. *J. Biol. Chem. 267*, 6164–6170.

8. Dahlbäck, B., and Villoutreix, B. O. (2005) The anticoagulant protein C pathway. *FEBS Lett. 579*, 3310–3316.
9. Koeppe, J. R., Seitova, A., Mather, T., and Komives, E. A. (2005) Thrombomodulin tightens the thrombin active site loop to promote protein C activation. *Biochemistry 44*, 14784–14791.
10. Walker, F. J., and Fay, P. J. (1992) Regulation of blood coagulation by the protein C system. *FASEB J. 6*, 2561–2567.
11. Gettins, P. G. W. (2002) Serpin structure, mechanism, and function. *Chem. Rev. 102*, 4751–4803.
12. Gandhi, P. S., Chen, Z., Mathews, F. S., and Di Cera, E. (2008) Structural identification of the pathway of long-range communication in an allosteric enzyme. *Proc. Natl. Acad. Sci. U.S.A. 105*, 1832–1837.
13. Stubbs, M. T., and Bode, W. (1993) A player of many parts: The spotlight falls on thrombin's structure. *Thromb. Res. 69*, 1–58.
14. Stearns, D. J., Kurosawa, S., and Esmon, C. T. (1989) Microthrombomodulin: Residues 310−486 from the epidermal growth factor precursor homology domain of thrombomodulin will accelerate protein C activation. *J. Biol. Chem. 264*, 3352–3356.
15. Fuentes-Prior, P., Iwanaga, Y, Huber, R., Pagila, R., Rumennik, G., Seto, M., Morser, J., Light, D. R., and Bode, W. (2000) Structural basis for the anticoagulant activity of the thrombin-thrombomodulin complex. *Nature 404*, 518–525.
16. Knobe, K., Berntsdotter, A., Shen, L., Morser, J., Dahlbäck, B., and Villoutreix, B. O. (1999) Probing the activation of protein C by the thrombin-thrombomodulin complex using structural analysis, site-directed mutagenesis, and computer modeling. *Proteins 35*, 218–234.
17. Zushi, M., Gomi, K., Yamamoto, S., Maruyama, I., Hayashi, T., and Suzuki, K. (1989) The last three consecutive epidermal growth factor-like structures of human thrombomodulin comprise the minimum functional domain for protein C-activating cofactor activity and anticoagulant activity. *J. Biol. Chem. 264*, 10351–10353.
18. Bode, W., Mayr, I., Baumann, U., Huber, R., Stone, S. R., and Hofsteenge, J. (1989) The refined 1.9 Å crystal structure of human α-thrombin: interaction with D-Phe-Pro-Arg chloromethylketone and significance of the Tyr-Pro-Pro-Trp insertion segment. *EMBO J. 8*, 3467–3475.
19. Schechter, I., and Berger, A. (1967) On the size of the active site in proteases. I. Papain. *Biochem. Biophys. Res. Commun. 27*, 157–162.
20. Zhang, E., and Tulinsky, A. (1997) The molecular environment of the Na^+ binding site of thrombin. *Biophys. Chem. 63*, 185–200.
21. Rezaie, A. R., and He, X. (2000) Sodium binding site of factor Xa: Role of sodium in the prothrombinase complex. *Biochemistry 39*, 1817–1825.
22. He, X., and Rezaie, A. R. (1999) Identification and characterization of the sodium-binding site of activated protein C. *J. Biol. Chem. 274*, 4970–4976.
23. Guinto, E. R., Caccia, S., Rose, T., Futterer, K., Waksman, G., and Di Cera, E. (1999) Unexpected crucial role of residue 225 in serine proteases. *Proc. Natl. Acad. Sci. U.S.A. 96*, 1852–1857.
24. Camire, R. M. (2002) Prothrombinase assembly and S1 site occupancy restore the catalytic activity of FXa impaired by mutation at the sodium-binding site. *J. Biol. Chem. 277*, 37863–37870.
25. Padmanabhan, K., Padmanabhan, K. P., Tulinsky, A., Park, C. H., Bode, W., Huber, R., Blankenship, D. T., Cardin, A. D., and Kisiel, W. (1993) Structure of human des (1−45) factor Xa at 2.2 Å resolution. *J. Mol. Biol. 232*, 947–966.
26. Mather, T., Oganessyan, V., Hof, P., Huber, R., Foundling, S., Esmon, C, and Bode, W. (1996) The 2.8 Å crystal structure of Gla-domainless activated protein C. *EMBO J. 15*, 6822–6831.
27. Bode, W., and Schwager, P. (1975) The refined crystal structure of bovine beta-trypsin at 1.8 Å resolution. II. Crystallographic refinement, calcium binding site, benzamidine binding site and active site at pH 7.0. *J. Mol. Biol. 98*, 693–717.
28. Rezaie, A. R., Mather, T., Sussman, F., and Esmon, C. T. (1994) Mutation of Glu 80 [to] Lys results in a protein C mutant that no longer requires Ca^{2+} for rapid activation by the thrombin-thrombomodulin complex. *J. Biol. Chem. 269*, 3151–3154.
29. Rezaie, A. R., and Esmon, C. T. (1994) Asp-70 to Lys mutant of factor X lacks the high affinity Ca^{2+} binding site yet retains function. *J. Biol. Chem. 269*, 21495–21499.
30. Rezaie, A. R., He, X., and Esmon, C. T. (1998) Thrombomodulin increases the rate of thrombin inhibition by BPTI. *Biochemistry 37*, 693–699.
31. Rezaie, A. R., and Yang, L. (2003) Thrombomodulin allosterically modulates the activity of the anticoagulant thrombin. *Proc. Natl. Acad. Sci. U.S.A. 100*, 12051–12056.
32. Gibbs, C. S., Coutré, S. E., Tsiang, M., Li, W. X., Jain, A. K., Dunn, K. E., Law, V. S., Mao, C. T., Matsumura, S. Y., Mejza, S. J., Paborsky, L. R., and Leung, L. L. K. (1995) Conversion of thrombin into an anticoagulant by protein engineering. *Nature 378*, 413–416.
33. Carter, W. J., Myles, T., Gibbs, C. S., Leung, L. L., and Huntington, J. A. (2004) Crystal Structure of anticoagulant thrombin variant E217K provides insights into thrombin allostery. *Biol. Chem. 279*, 26387–26394.
34. Ye, J., Esmon, N. L., Esmon, C. T., and Johnson, A. E. (1991) The active site of thrombin is altered upon binding to thrombomodulin: Two distinct structural changes are detected by fluorescence, but only one correlates with protein C activation. *J. Biol. Chem. 266*, 23016–23021.
35. Yang, L., Manithody, C., and Rezaie, A. R. (2006) Activation of protein C by the thrombin-thrombomodulin complex: Cooperative roles of Arg-35 of thrombin and Arg-67 of protein C. *Proc. Natl. Acad. Sci. U.S.A. 103*, 879–884.
36. Rezaie, A. R. (1996) Tryptophan60-D in the B-insertion loop of thrombin modulates the thrombin-antithrombin reaction. *Biochemistry 35*, 1918–1924.
37. Rezaie, A. R. (1998) Reactivities of the S2 and S3 subsite residues of thrombin with the native and heparin-induced conformers of antithrombin. *Protein Sci. 7*, 349–357.
38. Baerga-Ortiz, A., Rezaie, A. R., and Komives, E. A. (2000) Electrostatic dependence of the thrombin-thrombomodulin interaction. *J. Mol. Biol. 290*, 651–658.
39. Rezaie, A. R., and Esmon, C. T. (1992) The function of calcium in protein C activation by thrombin and the thrombin-thrombomodulin complex can be distinguished by mutational analysis of protein C derivatives. *J. Biol. Chem. 267*, 26104–26109.
40. Anderson, P. J., Nesset, A., Dharmawardana, K. R., and Bock, P. E. (2000) Role of proexosite I in factor Va-dependent substrate interactions of prothrombin activation. *J. Biol. Chem. 275*, 16435–16442.
41. Pineda, A. O., Carrell, C. J., Bush, L. A., Prasad, S., Caccia, S., Chen, Z.-W., Mathews, F. S., and Di Cera, E. (2004) Molecular dissection of Na^+ binding to thrombin. *J. Biol. Chem. 279*, 31842–31853.
42. Yang, L., Prasad, S., Di Cera, E., and Rezaie, A. R. (2004) The conformation of the activation peptide of protein C is influenced by Ca^{2+} and Na^+ binding. *J. Biol. Chem. 279*, 38519–38524.
43. Yang, L., Manithody, C., and Rezaie, A. R. (2002) Localization of the heparin binding exosite of factor IXa. *J. Biol. Chem. 277*, 50756–50760.
44. Bock, P. E. (1988) Active site selective labeling of serine proteases with spectroscopic probes using thioester peptide chloromethyl ketones: Demonstration of thrombin labeling using N^{α}-[(acetylthio)acetyl]-D-Phe-Pro-Arg-CH_2Cl. *Biochemistry 27*, 6633–6639.
45. Rezaie, A. R., and Olson, S. T. (1997) Contribution of Lysine 60f to S1' specificity of thrombin. *Biochemistry 36*, 1026–1033.
46. Humphrey, W., Dalke, A., and Schulten, K. (1996) VMD: visual molecular dynamics. *J. Mol. Graph. 14*, 33–38.
47. Kale, L., Skeel, R., Bhandarkar, M., Brunner, R., Gursoy, A., Krawetz, N., Philips, J., Shinozaki, A., Varadarajan, K., and Schulten, K. (1999) NAMD2: greater scalability for parallel molecular dynamics. *J. Comput. Phys. 151*, 283–312.
48. Jorgensen, W. L., Chandrashekhar, J., Madura, J. D., Impey, R. W., and Klein, M. L. (1983) Comparison of simple potential functions for simulating liquid water. *J. Chem. Phys. 79*, 926–935.
49. Darden, T., York, D., and Pedersen, L. (1993) An N.log(N) method for Ewald sums in large systems. *J. Chem. Phys. 98*, 10089–10092.
50. Essman, U., Perera, L., Berkowitz, M. L., Darden, T. A., Lee, H., and Pedersen, L. G. (1995) A smooth particle mesh Ewald method. *J. Chem. Phys. 103*, 8577–8592.
51. MacKerel, A. D. Jr., Bashford, D., Bellot, M., Dunbrack, R. L. Jr., Evanseck, J. D., Field, M. J., Fischer, S., Gao, J., Guo, H., Ha, S., Joseph-McCarthy, D., Kuchnir, L., Kuczera, K., Lau, F. T. K., Mattos, C., Michnick, S., Ngo, T., Nguyen, D. T., Prodhom, B., Reiher, W. E.III, Roux, B., Schlenkrich, M., Smith, J. C., Stote, R., Straub, J., Watanabe, M., Wiorkiewicz-Kuczera, J., Yin, D., and Karplus, M. (1998) All-atom empirical potential for molecular modeling and dynamics studies of proteins. *J. Phys. Chem. 102*, 3286–3616.
52. Pettersen, E. F., Goddard, T. D., Huang, C. C., Couch, G. S., Greenblatt, D. M., Meng, E. C., and Ferrin, T. E. (2004) UCSF Chimera: A visualization system for exploratory research analysis. *J. Comput. Chem. 25*, 1605–1612.
53. Yang, L., and Rezaie, A. R. (2003) The fourth epidermal growth factor-like domain of thrombomodulin interacts with the basic exosite of protein C. *J. Biol. Chem. 278*, 484–10490.
54. Pineda, A. O., Cantwell, A. M., Bush, L. A., Rose, T., and Di Cera, E. (2002) The thrombin epitope recognizing thrombomodulin is highly cooperative hot spot in exosite I. *J. Biol. Chem. 277*, 32015–32019.

55. Olson, S. T., Halvorson, H. R., and Bjork, I. (1991) Quantitative characterization of the thrombin-heparin interaction. Discrimination between specific and nonspecific binding models. *J. Biol. Chem. 266*, 6342–6352.
56. Anderson, P. J., Nesset, A., and Bock, P. E. (2003) Effects of activation peptide bond cleavage and fragment 2 interaction on the pathway of exosite 1 expression during activation of human prethrombin 1 to thrombin. *J. Biol. Chem. 278*, 44482–44488.
57. Bah, A., Garvey, L. C., Ge, J., and Di Cera, E. (2006) Rapid kinetics of Na^+ binding to thrombin. *J. Biol. Chem. 281*, 40049–40056.
58. Di Cera, E., Guinto, E. R., Vindigni, A., Dang, Q. D., Ayala, Y. M., Wuyi, M., and Tulinsky, A. (1995) The Na^+ binding site of thrombin. *J. Biol. Chem. 270*, 22089–22092.
59. Bush-Pelc, L. A., Marino, F., Chen, Z., Pineda, A. O., Mathews, F. S., and Di Cera, E. (2007) Important role of the cys-191 cys-220 disulfide bond in thrombin function and allostery. *J. Biol. Chem. 282*, 27165–27170.
60. Mutucumarana, V. P., Duffy, E. J., Lollar, P., and Johnson, A. E. (1992) The active site of factor IXa is located far above the membrane surface and its conformation is altered upon association with factor VIIIa: A fluorescence study. *J. Biol. Chem. 267*, 17012–17021.
61. Bah, A., Chen, Z., Bush-Pelc, L. A., Mathews, F. S., and Di Cera, E. (2007) crystal structures of murine thrombin in complex with the extracellular fragments of murine protease-activated receptors PAR3 and PAR4. *Proc. Natl. Acad. Sci. U.S.A. 104*, 11603–11608.
62. Fredenburgh, J. C., Stafford, A. R., and Weitz, J. (1997) Evidence for allosteric linkage between exosites 1 and 2 of thrombin. *J. Biol. Chem. 272*, 25493–25499.
63. Verhamme, I. M., Olson, S. T., Tollefsen, D. M., and Bock, P. E. (2002) Binding of exosite ligands to human thrombin. Re-evaluation of allosteric linkage between thrombin exosite I and II. *J. Biol. Chem. 277*, 6788–6798.
64. Arni, R. K., Padmanabhan, K., Padmanabhan, K. P., Wu, T.-P., and Tulinsky, A. (1993) Structures of the noncovalent complexes of human and bovine prothrombin fragment 2 with human PPACK-thrombin. *Biochemistry 32*, 4727–4737.